Biorheology 50 (2013) 269–282
DOI 10.3233/BIR-130643
IOS Press



# Shear viscosity and nonlinear behavior of whole blood under large amplitude oscillatory shear

P.C. Sousa [a,*], J. Carneiro [a], R. Vaz [b], A. Cerejo [b], F.T. Pinho [c], M.A. Alves [a] and M.S.N. Oliveira [d]

[a] *Departamento de Engenharia Química, CEFT, Faculdade de Engenharia da Universidade do Porto, Porto, Portugal*
[b] *Departamento de Neurocirurgia, Hospital S. João, Porto, Portugal*
[c] *Departamento de Engenharia Mecânica, CEFT, Faculdade de Engenharia da Universidade do Porto, Porto, Portugal*
[d] *James Weir Fluids Laboratory, Department of Mechanical and Aerospace Engineering, University of Strathclyde, Glasgow, UK*

Received 22 July 2013
Accepted in revised form 25 September 2013

**Abstract.** We investigated experimentally the rheological behavior of whole human blood subjected to large amplitude oscillatory shear under strain control to assess its nonlinear viscoelastic response. In these rheological tests, the shear stress response presented higher harmonic contributions, revealing the nonlinear behavior of human blood that is associated with changes in its internal microstructure. For the rheological conditions investigated, intra-cycle strain-stiffening and intra-cycle shear-thinning behavior of the human blood samples were observed and quantified based on the Lissajous–Bowditch plots. The results demonstrated that the dissipative nature of whole blood is more intense than its elastic component. We also assessed the effect of adding EDTA anticoagulant on the shear viscosity of whole blood subjected to steady shear flow. We found that the use of anticoagulant in appropriate concentrations did not influence the shear viscosity and that blood samples without anticoagulant preserved their rheological characteristics approximately for up to 8 minutes before coagulation became significant.

Keywords: Whole blood rheology, shear viscosity, anticoagulant effect, large amplitude oscillatory shear (LAOS)

## 1. Introduction

The investigation of the rheological behavior of whole blood has a long historical record dating back to the first half of the 20th century, with most studies focusing on the characterization of the steady-shear viscosity [3,7,8,11,20–23]. In spite of the large number of rheological investigations reported in the literature, their impact on clinical practice is still modest.

*Address for correspondence: Dr. P.C. Sousa, Departamento de Engenharia Química, CEFT, Faculdade de Engenharia da Universidade do Porto, Rua Dr. Roberto Frias, 4200-465 Porto, Portugal. Tel.: +351 22 508 1404; Fax: +351 22 508 1449; E-mail: psousa@fe.up.pt.

Blood is a non-Newtonian fluid and exhibits a complex rheological behavior, such as shear-thinning viscosity and thixotropy, primarily due to the presence of and interaction between cellular elements, mainly the red blood cells (RBC), which are the most abundant component and whose mechanical properties are inherent to the microstructure characteristic of blood.

The rotational rheometer is the most commonly used equipment to measure the time, strain and shear rate dependent rheological behavior of blood [20], but alternative rheological techniques have also been explored. For instance, a capillary tube viscometer able to measure the whole blood viscosity within 2 min was developed by Kim et al. [15] and Alexy et al. [1] proposed an automated tube-type viscometer operating over a wide range of shear rates (1–1500 $s^{-1}$) for rapid and reproducible blood viscosity measurements. Also, an oscillating resonator probe placed into the tube for blood withdrawal was developed by Mark et al. [18] in order to perform bedside blood rheological measurements given its good sensitivity to changes in blood viscosity due to alterations in the plasma and protein concentrations. This device is disposable and allows a rapid test without adding anticoagulant to the blood sample.

The idea that the addition of anticoagulants to blood samples can dilute blood and affect the rheological properties has been a matter of ample debate [2,12,24,25]. In particular, there has been discussion on the proper concentration of anticoagulant that should be used to prevent coagulation and prevent interference between components [4]. The most frequently used anticoagulants in hemorheological investigations are ethylenediaminetetraacetic acid (EDTA), heparin and citrate, which may be in liquid or solid phase. In the guidelines for hemorheological measurements recommended by the International Society for Clinical Hemorheology, the EDTA anticoagulant is preferred, and heparin is reported to change hemorheological parameters to a higher degree than the remaining anticoagulants [2].

Blood is also reported to exhibit viscoelastic properties but these are far less quantified, since measurements under oscillatory flow are far from conclusive, in addition to being limited to the linear regime (small strain amplitude). In a recent study, Campo-Deaño et al. [6] were able to measure the viscoelastic moduli of whole human blood using passive microrheology, confirming its viscoelastic nature. Moreover, a recent study by Brust et al. [5] showed that even plasma exhibits viscoelastic properties under extensional flow with a relaxation time at 37°C of the order of 0.5 ms. On the other hand, under pure shear flow conditions, plasma reveals a Newtonian-like flow behavior with negligible viscoelasticity.

In this work, we focus on the measurement of the oscillatory shear rheology of healthy human whole blood samples in large amplitude oscillatory shear (LAOS), which was used to quantify the nonlinear viscoelastic response of whole blood. Due to the small elasticity of blood and equipment limitations, accurate measurements of linear viscoelasticity under small amplitude conditions, and in particular of the elastic storage modulus, were not possible. To complement the rheological characterization under oscillatory flow, we also measured the whole blood flow curve and investigated the effects of anticoagulants used during blood collection.

## 2. Theoretical basis of large amplitude oscillatory shear

In oscillatory shear measurements both stress ($\tau$) and strain ($\gamma$) vary with time (with one of them imposed and the other monitored) and the viscous and elastic components of a viscoelastic material can be measured simultaneously [9].

Given the wide range of strain amplitudes and frequencies encompassed by small and large oscillatory shear flows, different conditions are achieved probing the linear and nonlinear viscoelastic properties of complex fluids, respectively [13,14]. Furthermore, the nonlinear rheological response in LAOS can be correlated with the microstructure of the viscoelastic sample.

In strain-controlled LAOS tests, the imposed strain follows a sinusoidal evolution in time and the corresponding shear stress response measured is not necessarily sinusoidal, revealing the nonlinear behavior of the sample.

The sinusoidal strain input is given by:

$$\gamma(t) = \gamma_1 \sin(\omega t), \tag{1}$$

where $\omega$ is the angular frequency, $t$ is the time and $\gamma_1$ is the maximum strain deformation of the cycle. The shear stress response in a LAOS test can be given as a sum of higher harmonic contributions [10, 14,16]:

$$\tau(t) = \sum_{n:1,3,5,\ldots} \tau_n \sin(n\omega t + \delta_n) = \gamma_1 \sum_{n:1,3,5,\ldots} |G_n^*| \sin(n\omega t + \delta_n), \tag{2}$$

where $|G_n^*| = \sqrt{G_n' + G_n''}$ with $G_n^*$ being the complex moduli, $G_n'$ the storage moduli, $G_n''$ the loss moduli and $\delta_n$ the phase angles.

The higher harmonic contributions are the main responsible for the nonsinusoidal shape of the shear stress waveform, with the 3rd harmonic being the one that most affects it [14]. Moreover, the phase angle for the 3rd harmonic gives information about sample structure as documented elsewhere [13].

Ewoldt et al. [10] characterized the complex nonlinear response in LAOS measurements based on the analysis of Lissajous–Bowditch plots, allowing the distinction between elastic and viscous nonlinearities. In a Lissajous–Bowditch plot, it is possible to illustrate the cyclic variations of shear stress as a function of strain, or shear stress versus shear rate, which occur during an oscillatory shear experiment. For a purely viscous material, a Lissajous–Bowditch plot of shear stress as a function of strain shows a circular shape (shear rate and strain are out of phase, with an angle $\pi/2$) and for an elastic material, the same plot reveals a straight line (stress and strain are in phase). Furthermore, for a linear viscoelastic sample, the stress–strain plot is elliptical and a deviation from an elliptical shape indicates a nonlinear behavior of the test sample. In contrast, the shape of a Lissajous–Bowditch plot of shear stress versus shear rate is a straight line for a viscous sample and a circle for an elastic material.

In the framework described by Ewoldt et al. [10], the following variables were defined in order to quantify the nonlinear viscoelastic properties: the minimum strain elastic shear modulus or tangent modulus at $\gamma = 0$, $G_M'$; and the large strain elastic shear modulus or secant modulus evaluated at the maximum imposed strain ($\gamma = \gamma_1$), $G_L'$. These variables are defined as [16]:

$$G_M' = \left.\frac{\mathrm{d}\tau}{\mathrm{d}\gamma}\right|_{\gamma=0} = \frac{1}{\gamma_1} \sum_{n:1,3,5,\ldots} n\tau_n \cos(\delta_n) = \sum_{n:1,3,5,\ldots} nG_n', \tag{3}$$

$$G_L' = \left.\frac{\tau}{\gamma}\right|_{\gamma=\pm\gamma_1} = \frac{1}{\gamma_1} \sum_{n:1,3,5,\ldots} (-1)^{(n-1)/2} \tau_n \cos(\delta_n) = \sum_{n:1,3,5,\ldots} G_n'(-1)^{(n-1)/2}. \tag{4}$$

These properties can be determined graphically using the Lissajous–Bowditch plot $\tau(\gamma)$ or from the Fourier parameters of the higher harmonic stress contributions, by obtaining the coefficients, $G_n'$, the amplitudes, $\tau_n$, and the phase angles, $\delta_n$. Graphically, the minimum-strain modulus represents the slope of the tangent at $\gamma = 0$ and the large-strain modulus represents the slope of a straight line connecting the axes origin to the point where the strain is maximum [10].

The minimum-rate and large-rate dynamic viscosities, $\eta'_M$ and $\eta'_L$, respectively, can also be defined in a similar manner [16]:

$$\eta'_M = \left.\frac{\mathrm{d}\tau}{\mathrm{d}\dot{\gamma}}\right|_{\dot{\gamma}=0} = \frac{1}{\omega\gamma_1}\sum_{n:1,3,5,\ldots}(-1)^{(n-1)/2}n\tau_n\sin(\delta_n) = \frac{1}{\omega}\sum_{n:1,3,5,\ldots}nG''_n(-1)^{(n-1)/2}, \tag{5}$$

$$\eta'_L = \left.\frac{\tau}{\dot{\gamma}}\right|_{\dot{\gamma}=\pm\dot{\gamma}_1} = \frac{1}{\omega\gamma_1}\sum_{n:1,3,5,\ldots}\tau_n\sin(\delta_n) = \frac{1}{\omega}\sum_{n:1,3,5,\ldots}G''_n. \tag{6}$$

These two properties define the instantaneous viscosities at the smallest and at the largest shear rates, respectively. In a Lissajous–Bowditch plot of the form $\tau(\dot{\gamma})$, $\eta'_M$ represents the slope of the tangent at $\dot{\gamma} = 0$ and $\eta'_L$ the slope of a straight line connecting the axes origin to the point for which the shear rate is maximum.

Based on these variables, it is possible to define the strain-stiffening ratio [10]:

$$S(\omega,\gamma_1) = \frac{G'_L - G'_M}{G'_L} \tag{7}$$

and the shear-thickening ratio:

$$T(\omega,\gamma_1) = \frac{\eta'_L - \eta'_M}{\eta'_L}. \tag{8}$$

For $S > 0$, the material shows intra-cycle strain-stiffening, whereas $S < 0$ indicates intra-cycle strain-softening. For a linear elastic response, $S = 0$. Similarly, $T = 0$ represents a linear viscous response, and $T > 0$ corresponds to intra-cycle shear-thickening and $T < 0$ intra-cycle shear-thinning [10].

## 3. Experimental techniques

### *3.1. Blood withdrawal, storage and preparation*

Whole blood samples were collected by venepuncture from two healthy human volunteers, who had given their informed consent. The donors were a male and a female, with average hematocrit values of 41.6% and 41.3%, respectively. The procedure of blood withdrawal and storage followed the new guidelines for hemorheological techniques recommended by the International Society for Clinical Hemorheology [2] and the work was carried out at Hospital de S. João (Porto, Portugal) in compliance with its Ethics Committee for Health.

Sampling was done in a quiet environment at ambient temperature ($T = 20 \pm 2^{\circ}$C) after overnight fasting of the donors. Blood withdrawal was carried out after a 15 min resting period in the seated position. The sampling site was the antecubital vein, and the sampling was done within 90 s after the application of a tourniquet. Sterile 21 G needles and 3 ml vacuum tubes (BD plastic Vacutainers®) containing $K_2$EDTA (1.8 mg cm$^{-3}$) were used for blood collection. The first blood sample to be tested after collection remained in the EDTA tube at room temperature for 10 min prior to testing. The remaining samples were cooled down to 4°C and stored for a maximum of 4 h before testing. Moreover, before

testing each sample was allowed to rest for 10 min at room temperature in order to equilibrate the temperature, after which the rheological measurements were carried out at 37°C. All measurements were performed on the day of blood withdrawal.

### 3.2. Rheological measurements of whole blood

The steady-state and oscillatory shear rheology of whole blood samples were characterized using a rotational rheometer (Physica MCR301, Anton Paar) with a Peltier temperature control system. The minimum torque of the rheometer is 0.1 μNm, or 0.02 μNm when the direct strain oscillation module (DSO) is used. The torque accuracy is 0.2 μNm for the experiments performed, with the torque resolution being 1 nNm. The measurements were performed using a 50 mm diameter serrated plate–plate geometry, denoted as PP50, using a gap of $h = 1$ mm. The serrated plate has a structured roughness shape with orthogonal protuberances having 1 mm spacing in both directions. A plate–plate geometry delays the onset of inertial instabilities at the higher shear-rates of the measurement, especially if small gaps are used. The geometry is schematically presented in Fig. 1.

Each blood sample was pipetted directly from the collection tube and placed in the middle of the lower plate of the rheometer after gentle agitation of the tube in order to promote the homogeneity of the sample. After that, the upper plate of the rheometer was moved to the measuring position (1 mm of gap) and the blood sample filled the gap between both plates. Prior to measurement, the samples were allowed to rest in the measurement gap for an adequate time (of the order of 60 s) in order to reach the desired temperature. Moreover, all the measurements were done within 20 min.

For steady shear measurements, the blood sample was *agitated* for 30 s at a shear rate of $\dot{\gamma} = 300\ \mathrm{s}^{-1}$ prior to the measurement of each point, in order to promote the homogeneity of the blood sample. Using this protocol, which was employed similarly in other investigations [17,19], the influence of sedimentation of RBC upon each data point is reduced and the results obtained are independent of the measuring profile imposed on the shear rates.

For oscillatory shear measurements, we performed strain-controlled LAOS tests using the DSO module of the rotational rheometer in order to generate an accurate sinusoidal strain input, by applying an angular frequency sweep at a fixed strain amplitude value. Due to instrument limitations and the small elastic character of blood, it was not possible to measure accurately the storage modulus using small amplitude oscillatory shear (SAOS). In addition, the tendency of RBC to sediment during SAOS measurements because of the small amplitudes of deformation employed also renders these measurements impracticable. Hence, we focus on the nonlinear response of whole blood using large amplitude oscillatory shear (LAOS) and in particular, the framework proposed by Ewoldt et al. [10] discussed in Section 2 is used to define and analyze the nonlinear viscous and elastic responses of human blood. For these tests,

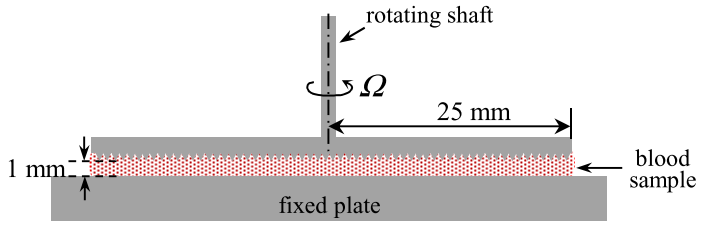


Fig. 1. Schematics of the measuring system used. The rotating part is on top and the fixed plate is positioned on bottom. The blood sample is placed in the gap between the lower plate and the upper fixture. The upper plate has a rough surface. (Colors are visible in the online version of the article; http://dx.doi.org/10.3233/BIR-130643.)

strain amplitudes of 10, 50 and 100 were imposed (the strain is defined as the ratio between the maximum amplitude of displacement of the periphery of the disk over the plate separation). All measurements under steady and oscillatory shear flow were performed at the physiological temperature, $T = 37°\mathrm{C}$.

## 4. Results and discussion

### *4.1. Influence of anticoagulant on the whole blood viscosity*

The steady-shear viscosity curve is presented in Fig. 2(a), where the shear-thinning character of blood is clearly visible. It is important to note that the results obtained in these measurements using blood samples from both donors are similar, since the hematocrit values are also similar.

A question that often arises is whether the use of the anticoagulant at the minimum admissible concentration to prevent coagulation (1.5–1.8 mg $\mathrm{cm}^{-3}$, as documented by Baskurt et al. [2]) affects or not the rheological behavior of whole blood. To clarify this issue, we measured the viscosity of whole blood samples with and without adding anticoagulant. As described in Section 3.1, blood samples were collected using Vacutainers® plastic tubes with EDTA for preventing blood coagulation during the rheological measurements, but when collecting blood without adding the EDTA anticoagulant we used a different procedure for blood withdrawal. Only in this case, blood was collected directly to a disposable plastic syringe, and transferred immediately to the rheometer in order to start the rheological measurement within the shortest possible time interval (typically within 2 min). In Fig. 2(b) we present a comparison between the flow curves measured for whole blood samples with and without the addition of EDTA anticoagulant. We used the maximum admissible concentration of the anticoagulant recommended by Baskurt et al. [2], which is 1.8 mg $\mathrm{cm}^{-3}$, to enhance the influence of anticoagulant as much as possible.

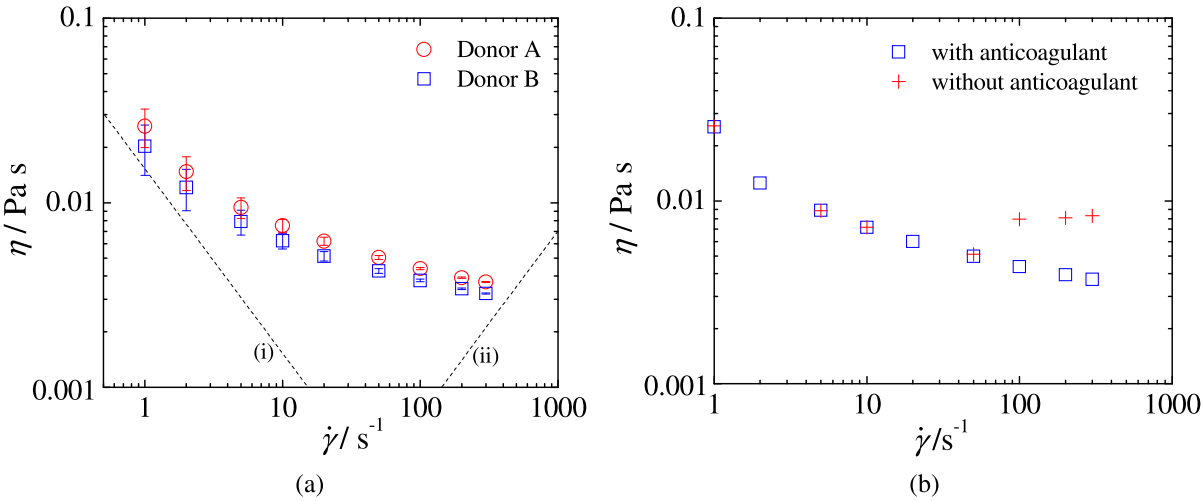


Fig. 2. (a) Steady-shear viscosity as a function of the shear rate measured at 37°C, for donor A (male) and donor B (female). The dashed lines represent the minimum measurable shear viscosity based on 5× the minimum resolvable torque (i) and the onset of secondary flow due to Taylor instabilities (ii). (b) Comparison of the steady-shear viscosity of whole blood samples from donor B measured at 37°C with and without adding anticoagulant. For both measurements, the shear rate was increased from 1 $\mathrm{s}^{-1}$ to 300 $\mathrm{s}^{-1}$. The shear viscosity of the blood sample without anticoagulant starts to deviate from that obtained with anticoagulant at $\dot{\gamma} = 100\ \mathrm{s}^{-1}$, approximately 8 min after blood collection, and presents higher values for this and the subsequent measurements at higher shear rates. (Colors are visible in the online version of the article; http://dx.doi.org/10.3233/BIR-130643.)

The results of the shear viscosity measurements for the sample containing the EDTA anticoagulant were similar to those of the blood sample without anticoagulant addition, with the differences between both measurements being within experimental uncertainty, at least during the first 8 min after blood collection. We observed that approximately 8–9 min after blood collection, the results obtained for the blood sample without anticoagulant start to deviate from those obtained using anticoagulant, probably due to the onset of blood coagulation.

### *4.2. Nonlinear viscoelastic behavior of blood*

We used LAOS tests to investigate the transient behavior of whole blood at large amplitude deformations. In Fig. 3(a1) and (b1) we present the strain waveforms imposed on the blood samples. The corresponding raw shear stress response measured over a period of one cycle is shown in Fig. 3(a2) and (b2), for blood samples from both donors. The corresponding Lissajous–Bowditch plots for $\gamma_1 = 10$ and $\omega = 0.158$ rad s$^{-1}$ are exhibited in Fig. 4.

The imposed strain waveform is sinusoidal, but the shear stress measured deviates clearly from a perfect sinusoidal function. A Fourier transform shows higher harmonic contributions as we can notice in Fig. 3(a2) for $\gamma_1 = 10$ ($t_{\text{period}} \approx 9$ s). When the sample deformation is increased to $\gamma_1 = 100$, the shape of the stress waveform changes and approaches a sinusoidal function, which is out of phase by $\pi/2$ relative to the imposed strain (Fig. 3(b2)). Changes in the shape of the shear stress waveform can be associated with alterations in the internal microstructure of human blood. A possible explanation for such alteration in the stress waveform output, for $\gamma_1 = 10$, is that RBC can aggregate, at least to a small extent, leading to the formation of weak structures when the deformation is smaller, but these structures tend to break when subject to higher deformations. Since at high deformations (and consequently deformation rates) RBC do not form aggregates, the shape of the observed shear stress output is closer to a perfect sinusoidal function. A similar phenomenon was observed with complex fluids of polymeric solutions, in which polymer chains can associate together [13].

Figure 4 shows the Lissajous–Bowditch plots of $\tau(\gamma)$ and $\tau(\dot{\gamma})$ for $\gamma_1 = 10$ and $\omega = 0.158$ rad s$^{-1}$ as well as $\gamma_1 = 100$ and $\omega = 1$ rad s$^{-1}$. In addition, the elastic moduli and dynamic viscosities defined in Section 2 are also illustrated in Fig. 4 and the corresponding values are presented in Table 1.

The rheological behavior observed for both donors, female and male, was similar. We verified that intra-cycle strain-stiffening ($S > 0$) occurs for all strain amplitudes investigated. Moreover, except only for blood samples from one donor at $\gamma_1 = 10$ and $\omega = 0.251$ rad s$^{-1}$, we verify that $\eta'_M > \eta'_L$, confirming the intra-cycle shear-thinning behavior.

The intra-cycle behavior for whole blood can be analyzed by means of normalized Lissajous–Bowditch plots in terms of shear stress versus strain and shear stress versus shear rate as displayed in Figs 5 and 6 for donors A and B, respectively. Data are normalized using the base wave or similarly, the first harmonic.

For a constant value of the angular frequency, the shape of the Lissajous–Bowditch plots for the higher strain amplitudes ($\gamma_1 = 50$ and 100) is very similar, but different from that at lower strain amplitude ($\gamma_1 = 10$). At the lower frequencies, i.e. slow deformation, the shape of the $\tau(\gamma)$ Lissajous–Bowditch plots for $\gamma_1 = 50$ and 100 is close to a circle indicating an essentially viscous behavior, whereas for the lower strain a distorted ellipse appears, with bent-elbow shape at the maximum and minimum strains, which is synonymous of simultaneous viscous and elastic behavior. On the other hand, the $\tau(\dot{\gamma})$ Lissajous–Bowditch plots show a nonelliptical shape with a small area enclosed for the higher strain amplitudes, while for $\gamma_1 = 10$ the internal area increases significantly. Considering for instance,

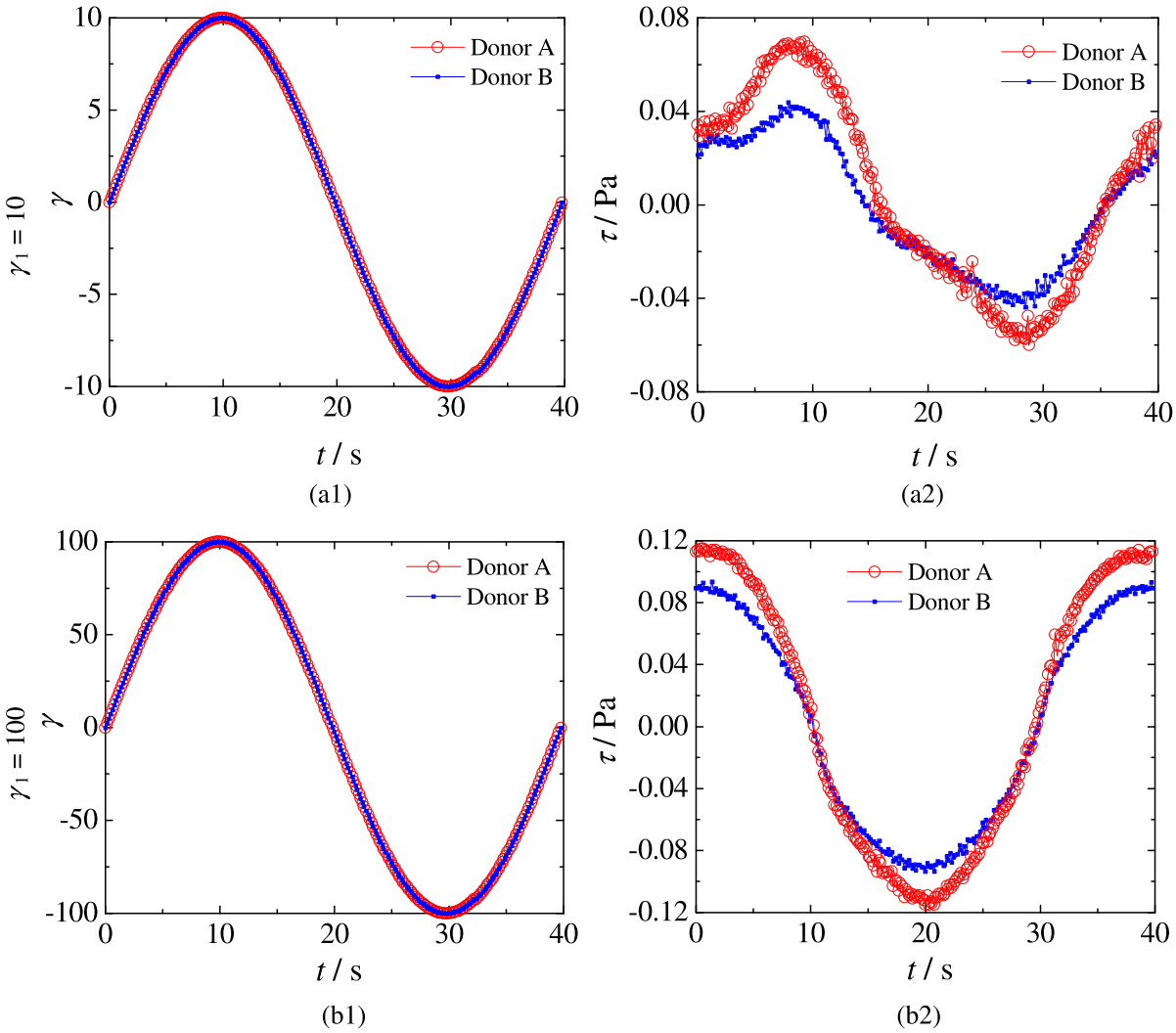


Fig. 3. Imposed strain waveform (*left column*) and shear stress waveform response (*right column*) at constant angular frequency $\omega = 0.158$ rad s$^{-1}$ for two different strain amplitudes, $\gamma_1 = 10$ (a) and 100 (b), and for blood donors A and B. (Colors are visible in the online version of the article; http://dx.doi.org/10.3233/BIR-130643.)

$\gamma_1 = 50$ and an angular frequency $\omega = 0.1$ rad s$^{-1}$, since the shape of the Lissajous–Bowditch plot $\tau(\gamma)$ is nearly circular and the inner area of that figure represents the lost energy, it is possible to associate a dominant viscous character to blood rheology. The weakly elastic nature of blood at small frequencies is further attested by the small enclosed area in the $\tau(\dot{\gamma})$ plot, which is proportional to the stored energy. Nevertheless, the small area observed demonstrates that whole human blood shows a slight elastic component under these rheological conditions, instead of a purely viscous character that would be anticipated by the nearly circular shape of the $\tau(\gamma)$ Lissajous–Bowditch plot.

Increasing the angular frequency, the Lissajous–Bowditch plots become more elliptical. However, we note that the shape of the figures is not a well-defined ellipse since we are outside the linear viscoelastic regime. Moreover, a visual inspection of the Lissajous–Bowditch plots shows that at lower $\gamma_1$ the area of

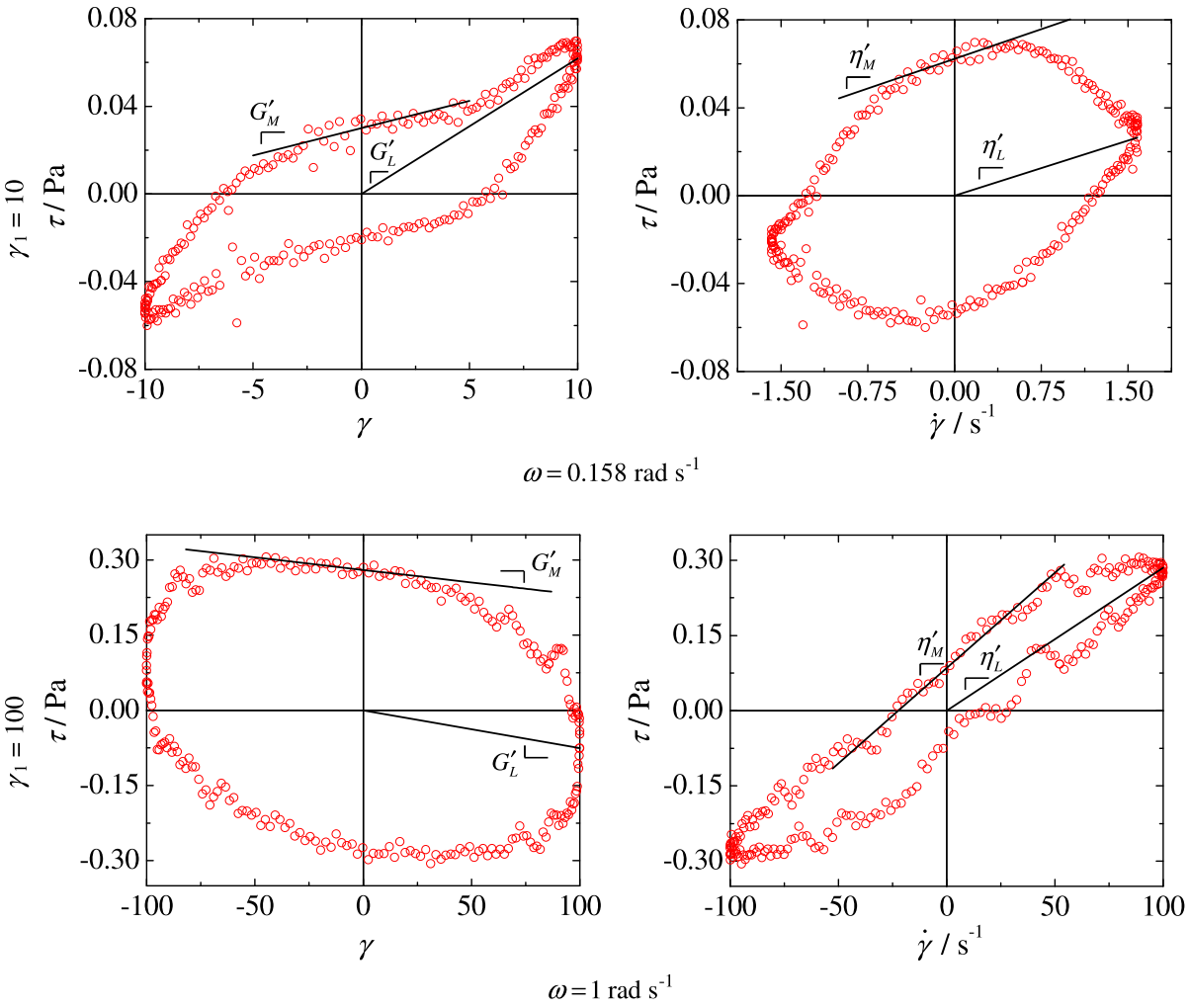


Fig. 4. Lissajous–Bowditch plots for two different strain amplitudes and angular velocities. The slopes of the lines represent the variables $G'_M$, $G'_L$, $\eta'_M$ and $\eta'_L$. Blood samples from donor A. (Colors are visible in the online version of the article; http://dx.doi.org/10.3233/BIR-130643.)

Table 1

Elastic moduli ($G'_M$ and $G'_L$), dynamic viscosities ($\eta'_M$ and $\eta'_L$) and dimensionless indices of nonlinearity ($S$ and $T$) calculated for two different amplitudes and angular velocities using the Fourier coefficients

| | $G'_M$ (Pa) | $G'_L$ (Pa) | $S$ | $\eta'_M$ (Pa s) | $\eta'_L$ (Pa s) | $T$ |
|---|---|---|---|---|---|---|
| $\gamma_1 = 10$ $\omega = 0.158$ rad s$^{-1}$ | $2.50 \times 10^{-3}$ | $5.84 \times 10^{-3}$ | 0.572 | $1.77 \times 10^{-2}$ | $1.61 \times 10^{-2}$ | $-0.100$ |
| $\gamma_1 = 100$ $\omega = 1$ rad s$^{-1}$ | $-6.50 \times 10^{-4}$ | $-7.50 \times 10^{-4}$ | 0.133 | $4.04 \times 10^{-3}$ | $2.85 \times 10^{-3}$ | $-0.417$ |

*Note*: The values correspond to the rheological data presented in Fig. 4 (blood samples from donor A).

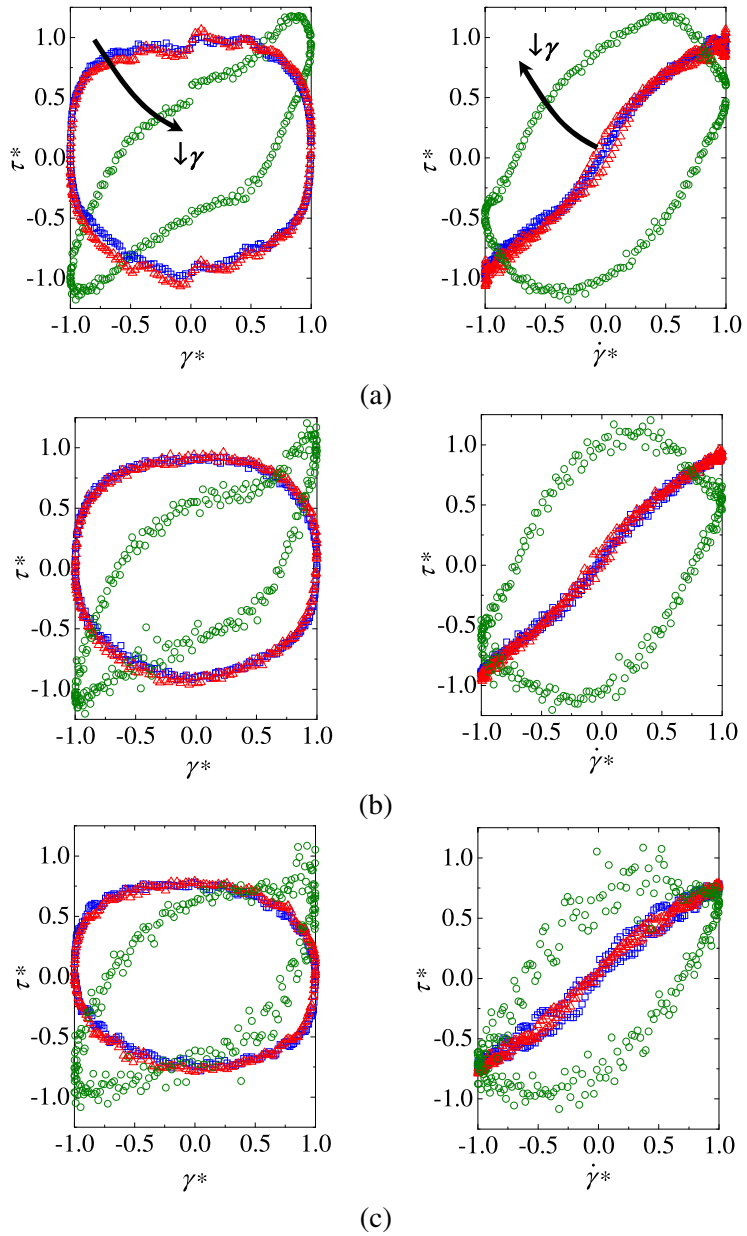


Fig. 5. Normalized Lissajous–Bowditch plots of shear stress as function of strain (left hand-side column) or shear rate (right hand-side column) at strain amplitudes of $\gamma_1 = 10$ (○), 50 (△) and 100 (□). The plots were obtained at different angular frequencies for blood donor A. The arrows indicate the direction of decreasing strain amplitude. (a) $\omega = 0.1$ rad s$^{-1}$. (b) $\omega = 0.251$ rad s$^{-1}$. (c) $\omega = 0.631$ rad s$^{-1}$. (d) $\omega = 3.98$ rad s$^{-1}$. (Colors are visible in the online version of the article; http://dx.doi.org/10.3233/BIR-130643.)

the $\tau(\gamma)$ figure decreases and that of $\tau(\dot{\gamma})$ increases, corresponding to a decrease of the dissipative energy and an increase of the stored energy [16]. However, they do not flatten significantly and consequently, human blood is far more dissipative than elastic in shear. We observe an increase of the storage energy with increasing angular frequency, indicative of the viscoelastic character of whole human blood.

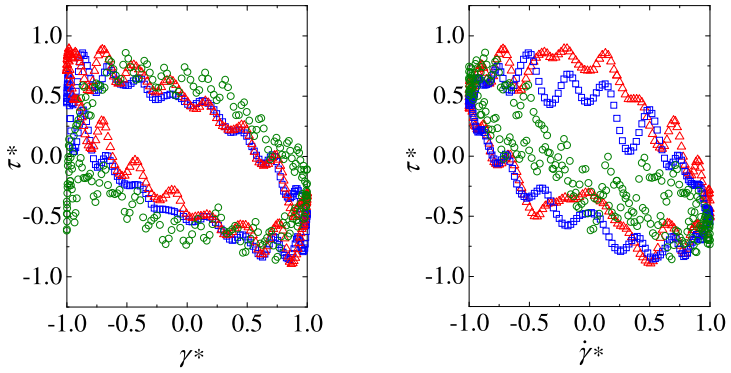


(d)

Fig. 5. (*Continued*). (Colors are visible in the online version of the article; http://dx.doi.org/10.3233/BIR-130643.)

It is worth noticing that when the angular frequency is increased, the layout of the Lissajous–Bowditch curve changes. Note that for the lower frequencies, $\partial\tau/\partial\dot{\gamma}$ is positive at, for instance $\dot{\gamma} = 0\ \mathrm{s}^{-1}$, while for the higher frequency, $\omega \approx 3.98$ rad $\mathrm{s}^{-1}$ (only shown in Fig. 5(d)), $\partial\tau/\partial\dot{\gamma}$ is negative at $\dot{\gamma} = 0\ \mathrm{s}^{-1}$. This phenomenon suggests that a dramatic change in the blood microstructure has taken place and this happens at $\omega \approx 2.5$ rad $\mathrm{s}^{-1}$ (not shown here). In addition, we observe some scatter and oscillations in the Lissajous–Bowditch plots at high frequencies (cf. Fig. 5(d)), which can be due to inertia related phenomena caused by the high rate of deformation used in these measurements. We also verify from the Fourier transform analysis that, for the angular velocity at which these oscillations are visible, the Fourier coefficients obtained and used to calculate the rheological properties do not have physical meaning. Furthermore, for those frequencies, it is not possible to represent graphically in the Lissajous–Bowditch plots the elastic moduli and dynamic viscosities obtained from the values of the odd-harmonic Fourier coefficients, because such values do not correspond to these measures. For all cases investigated, we compared the graphical representation of the rheological properties with the values obtained from the FT framework and the results showed good agreement, except when the Lissajous–Bowditch plots present the mentioned oscillations and the layout of the curve changes.

## 5. Conclusions

In the present work, we investigated the rheological properties of whole blood in steady and large amplitude oscillatory shear flow. The flow curves for blood samples with and without EDTA anticoagulant were also measured and we found the results were similar, indicating the negligible effect of EDTA on blood rheology. Moreover, the results show that blood samples without anticoagulant can preserve their characteristics approximately for up to 8–9 min before coagulation when an abnormal viscosity increase takes place.

The large amplitude oscillatory shear measurements were employed to characterize the nonlinear behavior of human whole blood and the corresponding important variables were quantified. The results show that the viscous component prevails over the elastic component, although a small elastic character is clearly visible under certain conditions. This investigation uses two blood donors to provide quantitative information about the nonlinear viscoelastic behavior of the human blood. Future studies considering a larger population would be insightful to assess whether person to person variability in hematology influences these nonlinear viscoelastic quantities.

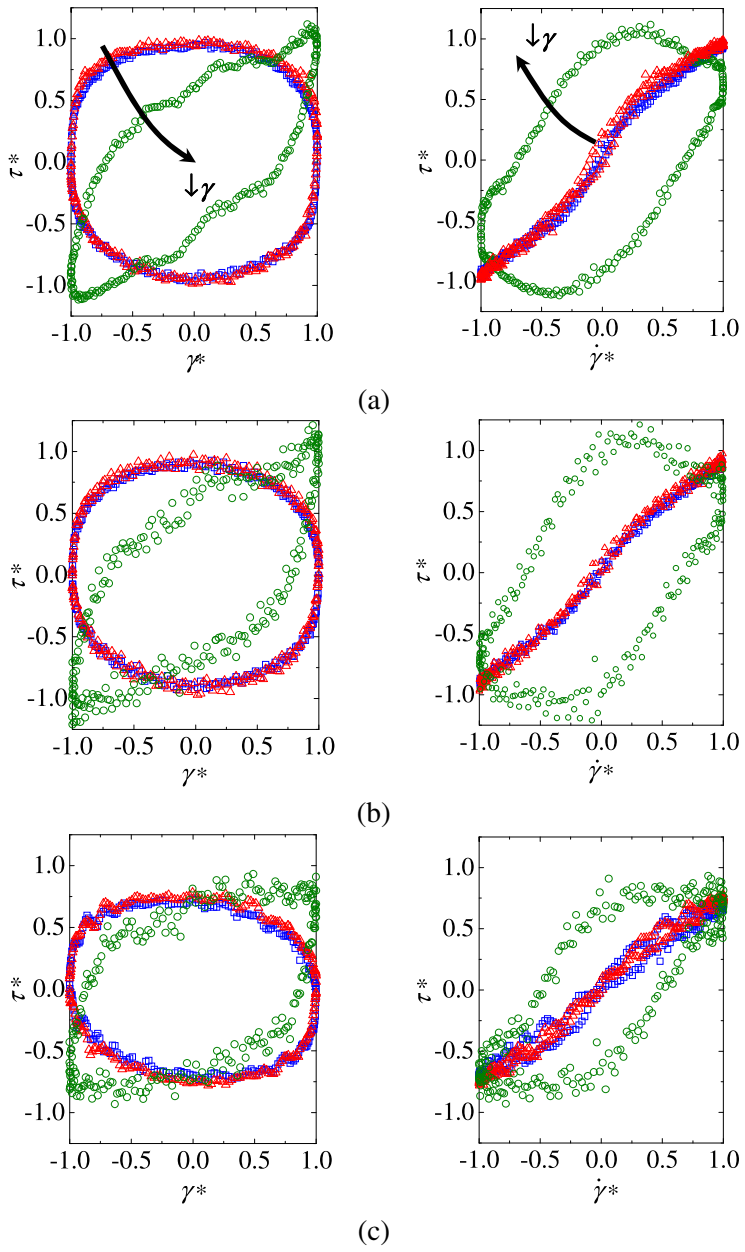


Fig. 6. Normalized Lissajous–Bowditch plots of shear stress as function of strain (left hand-side column) or shear rate (right hand-side column) at strain amplitudes of $\gamma_1 = 10$ (○), 50 (△) and 100 (□). The plots were obtained at different angular frequencies for blood donor B. The arrows indicate the direction of decreasing strain amplitude. (a) $\omega = 0.1$ rad s$^{-1}$. (b) $\omega = 0.251$ rad s$^{-1}$. (c) $\omega = 0.631$ rad s$^{-1}$. (Colors are visible in the online version of the article; http://dx.doi.org/10.3233/BIR-130643.)

## Acknowledgements

The authors acknowledge the financial support provided by Fundação para a Ciência e a Tecnologia (FCT) and FEDER through projects PTDC/EME-MFE/99109/2008, PTDC/SAU-BEB/105650/2008

and PTDC/EQU-FTT/118716/2010. P.C. Sousa would also like to thank FCT for financial support through scholarship SFRH/BPD/75258/2010. The help of the nursing staff, especially nurses Isabel Ribeiro and Rosa Silva, in the collection of blood samples and of Dr. Paulo Pinho are acknowledged. We also thank Thomas Ober and Chris Dimitriou for helpful discussions on LAOS, as well as Prof. Gareth McKinley and Prof. Randy Ewoldt for providing us with the MITlaos software.

## References

[1] T. Alexy, R.B. Wenby, E. Pais, L.J. Goldstein, W. Hogenauer and H.J. Meiselman, An automated tube-type blood viscometer: Validation studies, *Biorheology* **42** (2005), 237–247.
[2] O.K. Baskurt, M. Boynard, G.C. Cokelet, P. Connes, B.M. Cooke, S. Forconi et al., New guidelines for hemorheological laboratory techniques, *Clin. Hemorheol. Microcirc*. **42** (2009), 75–97.
[3] A.M. Benis and J. Lacoste, Study of erythrocyte aggregation by blood viscometry at low shear rates using a balance method, *Circ. Res*. **22** (1968), 29–42.
[4] R.A.R. Bowen, G.L. Hortin, G. Csako, O.H. Otanez and A.T. Remaley, Impact of blood collection devices on clinical chemistry assays, *Clin. Biochem*. **43** (2010), 4–25.
[5] M. Brust, C. Schaefer, R. Doerr, L. Pan, M. Garcia, P.E. Arratia and C. Wagner, Rheology of human blood plasma: Viscoelastic versus Newtonian behavior, *Phys. Rev. Lett.* **110** (2013), 078305–5.
[6] L. Campo-Deaño, R.P.A. Dullens, D.G.A.L. Aarts, F.T. Pinho and M.S.N. Oliveira, Viscoelasticity of blood and viscoelastic blood analogues for use in polydymethylsiloxane *in vitro* models of the circulatory system, *Biomicrofluidics* **7** (2013), 034102-11.
[7] S. Chien, Shear dependence of effective cell volume as a determinant of blood viscosity, *Science* **168** (1970), 977–979.
[8] S. Chien, S. Usami, H.M. Taylor, J.L. Lundberg and M.I. Gregerse, Effects of hematocrit and plasma proteins on human blood rheology at low shear rates, *J. Appl. Physiol*. **21** (1966), 81–87.
[9] A.P. Deshpande, Oscillatory shear rheology for probing nonlinear viscoelasticity of complex fluids: Large amplitude oscillatory shear, in: *Rheology of Complex Fluids*, A.P. Deshpande, J.M. Krishnan and S. Kumar, eds, Springer, New York, 2010, pp. 87–110.
[10] R.H. Ewoldt, A.E. Hosoi and G.H. McKinley, New measures for characterizing nonlinear viscoelasticity in large amplitude oscillatory shear, *J. Rheol*. **52** (2008), 1427–1458.
[11] R. Fåhræus, The suspension stability of the blood, *Physiol. Rev*. **9** (1929), 241–274.
[12] M. Hitosugi, M. Niwa and A. Takatsu, Changes in blood viscosity by heparin and argatroban, *Thromb. Res*. **104** (2001), 371–374.
[13] K. Hyun, J.G. Nam, M. Wilhelm, K.H. Ahn and S.J. Lee, Nonlinear response of complex fluids under LAOS (large amplitude oscillatory shear) flow, *Korea–Aust. Rheol. J*. **15** (2003), 97–105.
[14] K. Hyun, M. Wilhelm, C.O. Klein, K.S. Cho, J.G. Nam, K.H. Ahn et al., A review of nonlinear oscillatory shear tests: Analysis and application of large amplitude oscillatory shear (LAOS), *Progr. Polym. Sci*. **36** (2011), 1697–1753.
[15] S. Kim, Y.I. Cho, A.H. Jeon, B. Hogenauer and K.R. Kensey, A new method for blood viscosity measurement, *J. Non-Newton. Fluid Mech*. **94** (2000), 47–56.
[16] J. Läuger and H. Stettin, Differences between stress and strain control in the non-linear behavior of complex fluids, *Rheol. Acta* **49** (2010), 909–930.
[17] B.K. Lee, T. Alexy, R.B. Wenby and H.J. Meiselman, Red blood cell aggregation quantitated via Myrenne aggregometer and yield shear stress, *Biorheology* **44** (2007), 29–35.
[18] M. Mark, K. Häusler, J. Dual and W.H. Reinhart, Oscillating viscometer – Evaluation of a new bedside test, *Biorheology* **43** (2006), 133–146.
[19] Z. Marton, G. Kesmarky, J. Vekasi, A. Cser, R. Russai, B. Horvath and K. Toth, Red blood cell aggregation measurements in whole blood and in fibrinogen solutions by different methods, *Clin. Hemorheol. Microcirc*. **24** (2001), 75–83.
[20] C. Picart, J.M. Piau, H. Galliard and P. Carpentier, Human blood shear yield stress and its hematocrit dependence, *J. Rheol*. **42** (1998), 1–12.
[21] B. Pirofsky, The determination of blood viscosity in man by a method based on Poiseuille's law, *J. Clin. Invest*. **32** (1953), 292–298.
[22] G.B. Thurston, Rheological parameters for the viscosity, viscoelasticity and thixotropy of blood, *Biorheology* **16** (1979), 149–162.
[23] V. Travagli, I. Zanardi, L. Boschi, A. Gabbrielli, V.A.M. Mastronuzzi, R. Cappelli and S. Forconi, Comparison of blood viscosity using a torsional oscillation viscometer and a rheometer, *Clin. Hemorheol. Microcirc*. **38** (2008), 65–74.

[24] S. Wang, A.H. Boss, K.R. Kensey and R.S. Rosenson, Variations of whole blood viscosity using Rheolog™ a new scanning capillary viscometer, *Clin. Chem. Acta* **332** (2003), 79–82.
[25] S.R. Wickramasinghe and B. Han, Designing microporous hollow fibre blood oxygenators, *Chem. Eng. Res. Design* **83** (2005), 256–267.